Journal of Cardiovascular Emergencies 2026;12(3):122-131
DOI: 10.2478/jce-2026-0011

ORIGINAL RESEARCH

Development of Large-Diameter Tissue-Engineered Vascular Grafts as an Alternative to Synthetic Conduits for Emergency Large-Vessel Trauma Reconstruction: A Preliminary Study

Bogdan Ioan Lăpădatu[1], Constantin Claudiu Ciucanu[2,3], Alexandru Mureșan[3*], Paula Bândea[3], Petru Alexandru Ion[4], Emil-Marian Arbănași[2,3,5], Marius-Alexandru Beleaua[6], Réka Bartus[2,3], Adrian Vasile Mureșan[2,3], Eliza Russu[2,3,4]

[1] Faculty of General Medicine, George Emil Palade University of Medicine, Pharmacy, Science and Technology, Târgu Mureș, Romania
[2] Department of Vascular Surgery, George Emil Palade University of Medicine, Pharmacy, Science and Technology, Târgu Mureș, Romania
[3] Clinic of Vascular Surgery, Mures County Emergency Hospital, Târgu Mureș, Romania
[4] Doctoral School of Medicine and Pharmacy, George Emil Palade University of Medicine, Pharmacy, Science and Technology, Târgu Mureș, Romania
[5] Regenerative Medicine Laboratory, Center for Advanced Medical and Pharmaceutical Research (CCAMF), George Emil Palade University of Medicine, Pharmacy, Science and Technology, Târgu Mureș, Romania
[6] Department of Pathology, George Emil Palade University of Medicine, Pharmacy, Science and Technology, Târgu Mureș, Romania

ABSTRACT

Background: Major vascular trauma requires immediate restoration of perfusion, yet conduit options for large-vessel reconstruction are limited. Autologous veins are poorly matched to the caliber of the aorta and iliac arteries and may be unavailable in polytrauma, whereas synthetic grafts are biologically inert, prone to neointimal hyperplasia, and vulnerable to infection in contaminated fields. Decellularized xenogeneic scaffolds have been proposed as tissue-engineered vascular grafts (TEVGs) but remain underexplored for large-diameter applications. This study aimed to develop a rapid perfusion-based decellularization protocol for porcine aortic scaffolds, evaluate the effects of glutaraldehyde (GA) crosslinking, and characterize the resulting mechanical properties as a first step toward a large-diameter TEVG for emergency vascular reconstruction. **Material and Methods:** Twelve porcine thoracic aortic segments were processed into three paired groups: untreated, decellularized, and decellularized plus GA-crosslinked. Decellularization used recirculating perfusion with sequential 1% Triton X-100 and 1% sodium dodecyl sulfate and was confirmed by hematoxylin and eosin staining. **Results:** Decellularization significantly decreased the ultimate tensile stress compared to native tissue (4.09 ± 0.25 MPa vs. 5.34 ± 0.41 MPa, $p < 0.0001$) and also lowered Young's modulus ($p = 0.0024$), but it did not affect failure strain ($p = 0.7881$). GA crosslinking brought the ultimate stress back to levels similar to native tissue (5.16 ± 0.71 MPa, $p = 0.8352$) and increased Young's modulus beyond native values (5.93 ± 0.84 MPa, $p = 0.0005$), although it significantly reduced failure strain ($p = 0.0006$). Histological analysis confirmed complete nuclear removal with preserved fibrillar matrix structure. **Conclusions:** Rapid perfusion-

ARTICLE HISTORY

Received: June 1, 2026
Accepted: July 16, 2026

based decellularization followed by GA crosslinking yielded large-diameter porcine aortic scaffolds with tensile strength restored to native levels and increased stiffness, at the cost of reduced extensibility. These findings establish a biomechanical basis for further development of decellularized porcine aortic conduits as off-the-shelf large-diameter TEVGs, pending in vivo evaluation of remodeling, patency, and infection resistance.

Keywords: tissue-engineered vascular graft, bioengineering, biomechanics, vascular surgery, crosslinking

CORRESPONDENCE

Alexandru Mureșan
Email: alex.muresan99@yahoo.ro

INTRODUCTION

Traumatic vascular injury is a life- and limb-threatening emergency in which prompt restoration of perfusion is decisive for outcome; rapid decisions regarding hemorrhage control and limb-threatening ischemia directly determine survival and functional outcomes.[1] Vascular injuries predominantly result from penetrating mechanisms in urban settings and blunt trauma in rural areas, with the latter associated with higher mortality and limb amputation rates.[2] Anatomically, the extremities are involved in 44% of cases, followed by abdominal, thoracic, and cervical vessels.[3] Injuries to major vessels are particularly challenging, requiring rapid diagnosis, prompt hemorrhage control, and timely restoration of distal perfusion to improve survival and reduce limb loss.[1]

Endovascular techniques have seen growing adoption in vascular trauma management, with the clearest benefit demonstrated in blunt aortic injury, where stent graft repair offers procedural and outcome advantages over open surgery.[4,5] Studies have described endovascular treatment of arterial and venous injuries,[6,7] and these approaches are particularly valuable in anatomically challenging regions such as the thoracic aorta and subclavian artery, where hybrid or definitive stent graft repair may be favored.[3,8] However, the overall evidence base remains limited, and stent grafts may inadequately address local tissue damage and concomitant nerve or vein injuries, while raising concerns regarding long-term patency and durability.[4,5]

Conduit selection depends on injury location, wound contamination, and vessel caliber. Current trauma guidelines recommend autologous vein for smaller vessels and synthetic interposition grafts for emergency definitive repair of larger vessels.[1,9] The great saphenous vein is the preferred conduit for extremity injuries and remains the first choice when available, despite its susceptibility to thrombosis, intimal hyperplasia, atherosclerosis, and infection; its use, however, is effectively limited to small- and medium-caliber reconstruction.[10,11]

Although autologous vessels are generally preferred, their use in major vessel trauma is limited: the great saphenous vein is poorly matched to the diameter of the aorta and iliac arteries, harvesting a suitable conduit may delay revascularization in hemodynamically unstable patients, and previous surgery, anatomical variation, or associated injuries may further restrict autologous tissue availability.[12] In damage-control surgery and polytrauma, suitable autologous conduits may be unavailable or impractical to harvest because of associated extremity injuries, the need to minimize operative time, and hemodynamic instability, making immediate reconstruction reliant on readily available vascular substitutes.[13–15]

When autologous conduits are unavailable, artificial vascular grafts represent a practical alternative; the ideal graft must satisfy several requirements, including biocompatibility, adequate mechanical strength, appropriate permeability, and resistance to thrombosis.[12] Synthetic grafts, particularly expanded polytetrafluoroethylene (ePTFE) and polyethylene terephthalate (Dacron), are therefore commonly used when immediate reconstruction is required.[16] For larger diameters (>6 mm) these grafts are well established in clinical practice; however, they are biologically inert, undergo little physiological remodeling or endothelialization, and show reduced long-term patency owing to compliance mismatch and thrombus formation on the synthetic surface.[17]

Their principal mode of mid-term failure is neointimal hyperplasia (the accumulation of smooth-muscle cells and extracellular matrix within the intima) triggered by endothelial injury at implantation and compounded by compliance mismatch and anastomotic stress, ultimately producing luminal stenosis and distal ischemia.[12,18] Beyond these biological limitations, synthetic conduits must also meet biomechanical requirements such as sufficient elasticity, compliance, fatigue resistance, and suture retention strength.[19]

Synthetic grafts are also problematic in contaminated or infected fields. Prosthetic graft infection, typically arising from bacterial colonization, is a serious complication

that may cause thrombosis, anastomotic disruption, recurrent hemorrhage, or graft failure, and frequently requires surgical explantation, carrying substantial mortality and morbidity.[16,20,21]

The limitations of both autologous and synthetic conduits have driven interest in tissue-engineered vascular grafts (TEVGs), which aim to combine immediate availability with superior host integration and regenerative potential.[19-21] Decellularized xenogeneic scaffolds represent a compelling biological platform for this purpose: by selectively removing cellular components while preserving the native extracellular matrix architecture, they provide a structural template conducive to host cell infiltration, attachment, and tissue remodeling.[22-24] Their essentially unlimited availability and freedom from donor-site morbidity are additional practical advantages, and xenogeneic processing substantially attenuates the risk of immune or inflammatory responses.[22-24] Despite these properties, TEVGs have been developed predominantly as small-diameter substitutes,[25,26] and although decellularized human and porcine aortic tissues have shown promise as large-diameter scaffolds,[27-29] this application remains substantially underexplored relative to its potential clinical value in emergency and complex arterial reconstruction.[22,24,30,31]

This study therefore aimed to develop a rapid perfusion-based decellularization protocol for porcine aortic scaffolds, evaluate the effects of glutaraldehyde (GA) crosslinking, and characterize the resulting mechanical properties as a first step toward a large-diameter TEVG for emergency vascular reconstruction.

MATERIALS AND METHODS

All experimental procedures, including tissue harvesting, perfusion-based decellularization, glutaraldehyde crosslinking, and biomechanical testing, were performed in the Regenerative Medicine Laboratory at the Center for Advanced Medical and Pharmaceutical Research (CCAMF) in Târgu Mureș, Romania.

TISSUE HARVEST AND SPECIMEN PREPARATION

Twelve thoracic aortic segments were harvested from porcine donors from a local slaughterhouse and transported to the laboratory on ice for subsequent analysis within the first 6 h (Figure 1A).[32] Perivascular adipose and loose connective tissue were removed under sterile conditions, and each aorta was rinsed in phosphate buffer solution (PBS) to clear residual luminal blood. To reduce bias caused by regional and intersegment differences in the aortic wall, three adjacent specimens were taken side by side from the same aortic region of each donor. Each specimen was assigned to one of the three study groups: untreated control ('Native'), decellularized specimens ('Decell'), and decellularized specimens then crosslinked with glutaraldehyde ('Decell+GA').

PERFUSION DECELLULARIZATION

Perfusion-based decellularization was performed following the protocol described by Massaro *et al.*,[23] adapted for porcine thoracic aorta. Each aortic segment was ligated at both ends to Luer connectors with ligatures and incorporated into a recirculating perfusion circuit consisting of flexible tubing, a reservoir bottle containing the working solution, and a Masterflex L/S peristaltic pump (Cole-Parmer Instrument Co.) operated at a flow rate of 250 ml/min (Figure 1C, D). Solutions were perfused through the vessel lumen in the direction of physiological flow. Because the thoracic aortic wall is substantially thicker than the carotid artery for which the original protocol was developed, the number of detergent perfusion cycles was doubled to ensure complete decellularization. The protocol comprised an initial 10-min saline wash to clear residual blood, followed by four successive 1-h perfusion cycles with 1% Triton X-100, four successive 1-h cycles with 1% sodium dodecyl sulfate (SDS), and a final series of four cycles of 15 min of saline washes to remove residual detergent. All steps were conducted at room temperature under sterile conditions. Decellularization was indicated grossly by the transition from native vascularized tissue to an opaque, off-white acellular conduit with preserved tubular geometry (Figure 1E).

To confirm and validate the efficacy of decellularization, a 5-mm ring was excised from each conduit before and after processing and fixed in 10% neutral-buffered formalin. Paired native and decellularized samples were processed routinely, paraffin-embedded, and stained with hematoxylin and eosin (H&E). Sections were examined under light microscopy to assess the removal of cellular and nuclear material, with successful decellularization defined as the absence of intact nuclei within a preserved extracellular matrix architecture.

MECHANICAL TESTING

Uniaxial tensile testing to failure was performed using a CellScale BioTester 5000 (CellScale Biomaterials Testing) (Figure 1). Specimen thickness and width were measured using a digital thickness gauge (Mitutoyo 547-500S, Ka-

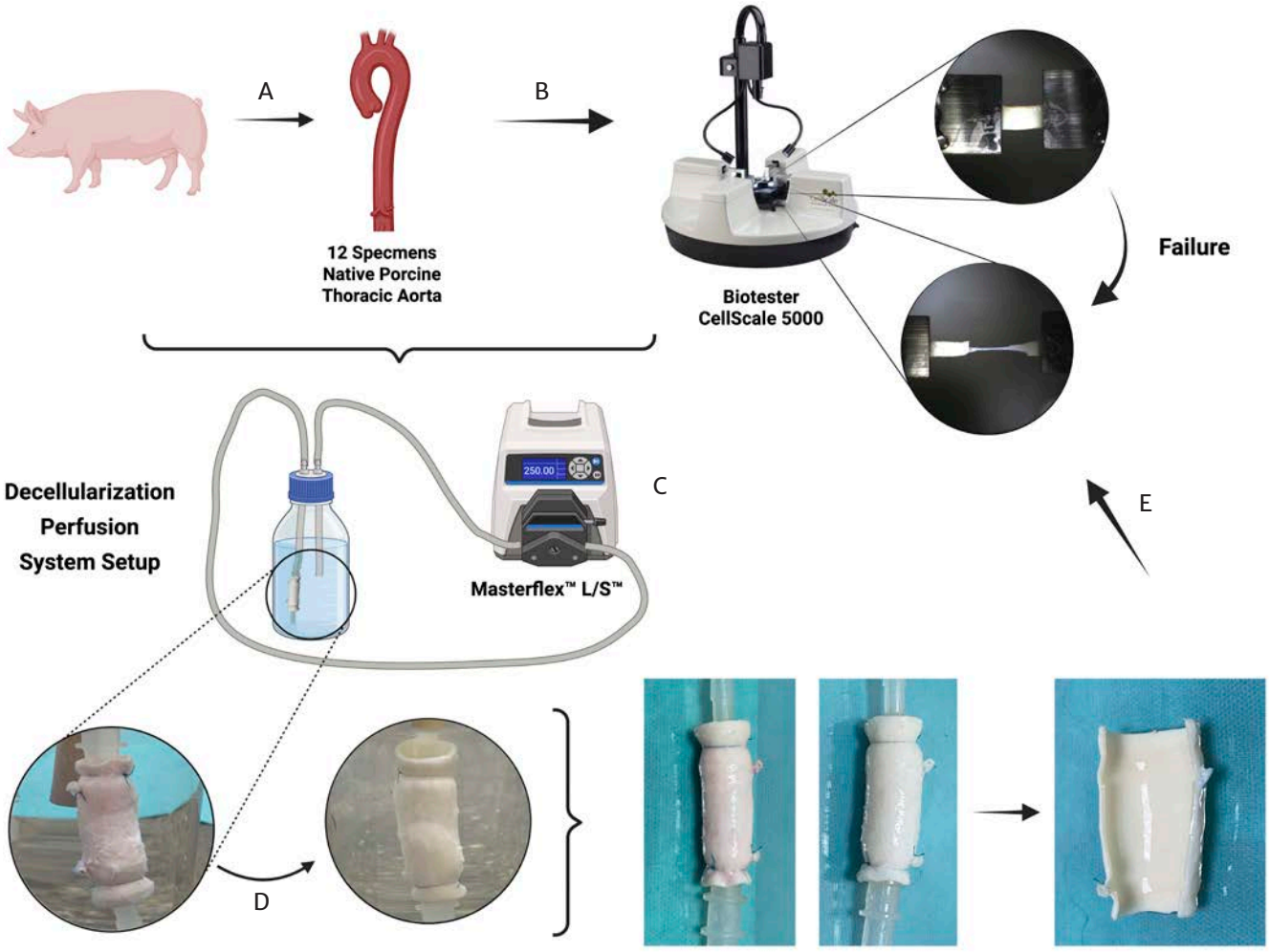

FIGURE 1. Workflow for the development of large-diameter tissue-engineered vascular grafts from porcine thoracic aorta, comprising tissue harvest (**A**), uniaxial tensile testing to failure (**B**), perfusion-based decellularization (**C**, **D**), and progression of the processed conduit to crosslinking and biomechanical evaluation (**E**).

wasaki) with a protocol validated previously.[33–35] Ultimate tensile stress, strain at failure, and Young's modulus, defined as the slope of the linear elastic region of the stress–strain curve, were calculated for each specimen according to the literature.[36,37] Mechanical testing and thickness measurement were performed with the operator/analyst blinded to group allocation; specimens were coded and tested in randomized order, and stress–strain parameters were computed from instrument output before decoding. Between harvest and testing, all specimens were kept hydrated in PBS and were never frozen. Native specimens were tested fresh within 6 h of harvest. Decellularized specimens were tested on completion of the perfusion protocol, following 1 h of equilibration in PBS. Decell+GA specimens were tested after 24 h of GA immersion and a subsequent PBS rinse. All mechanical testing was performed at room temperature.

GLUTARALDEHYDE CROSSLINKING

A subset of decellularized conduits was crosslinked by immersion in 0.6% GA solution for 24 h at room temperature. This concentration lies within the range established for clinical bioprosthetic tissue fixation and was selected to provide adequate collagen crosslinking while limiting the concentration-dependent cytotoxicity and calcification associated with higher GA exposure. Moreover, the 24-h immersion was chosen to ensure transmural penetration and uniform fixation of the full-thickness aortic wall.[38,39]

STATISTICAL ANALYSIS

Statistical analyses were performed using IBM SPSS software (IBM). Continuous variables are expressed as mean ± standard deviation. The normality of data distribution

TABLE 1. Biomechanical properties of native, decellularized, and glutaraldehyde-crosslinked porcine thoracic aorta

Biomechanical characteristics	Porcine aorta		
	Native	Decell	Decell+GA
Thickness (mm)	1.51 ± 0.15	1.37 ± 0.14	1.37 ± 0.09
Strain (%)	124.25 ± 11.61	121.25 ± 12.61	105.33 ± 8.83
Ultimate stress (MPa)	5.34 ± 0.41	4.09 ± 0.25	5.16 ± 0.71
Young's modulus (MPa)	4.96 ± 0.42	4.12 ± 0.25	5.93 ± 0.84

was assessed using the Shapiro–Wilk test. Comparisons among the three groups (Native, Decell, and Decell+GA) were performed using one-way analysis of variance (ANOVA) followed by Tukey's post hoc test for multiple pairwise comparisons. A two-sided p value of <0.05 was considered statistically significant.

RESULTS

The geometric and mechanical properties of all 12 specimens per group are summarized in Table 1.

Wall thickness decreased modestly but significantly after decellularization compared with native specimens (p = 0.0366), and this difference persisted after GA crosslinking (p = 0.0321) (Figure 2). Decellularization alone markedly reduced ultimate tensile stress relative to native tissue (p < 0.0001), whereas GA crosslinking reversed this deficit: ultimate stress in the Decell+GA group recovered to 5.16 ± 0.71 MPa, a value statistically indistinguishable from native aorta (p = 0.8352) and significantly higher than the decellularized-only group (p = 0.0008) (Figure 2). Stiffness and extensibility followed an inverse, crosslink-

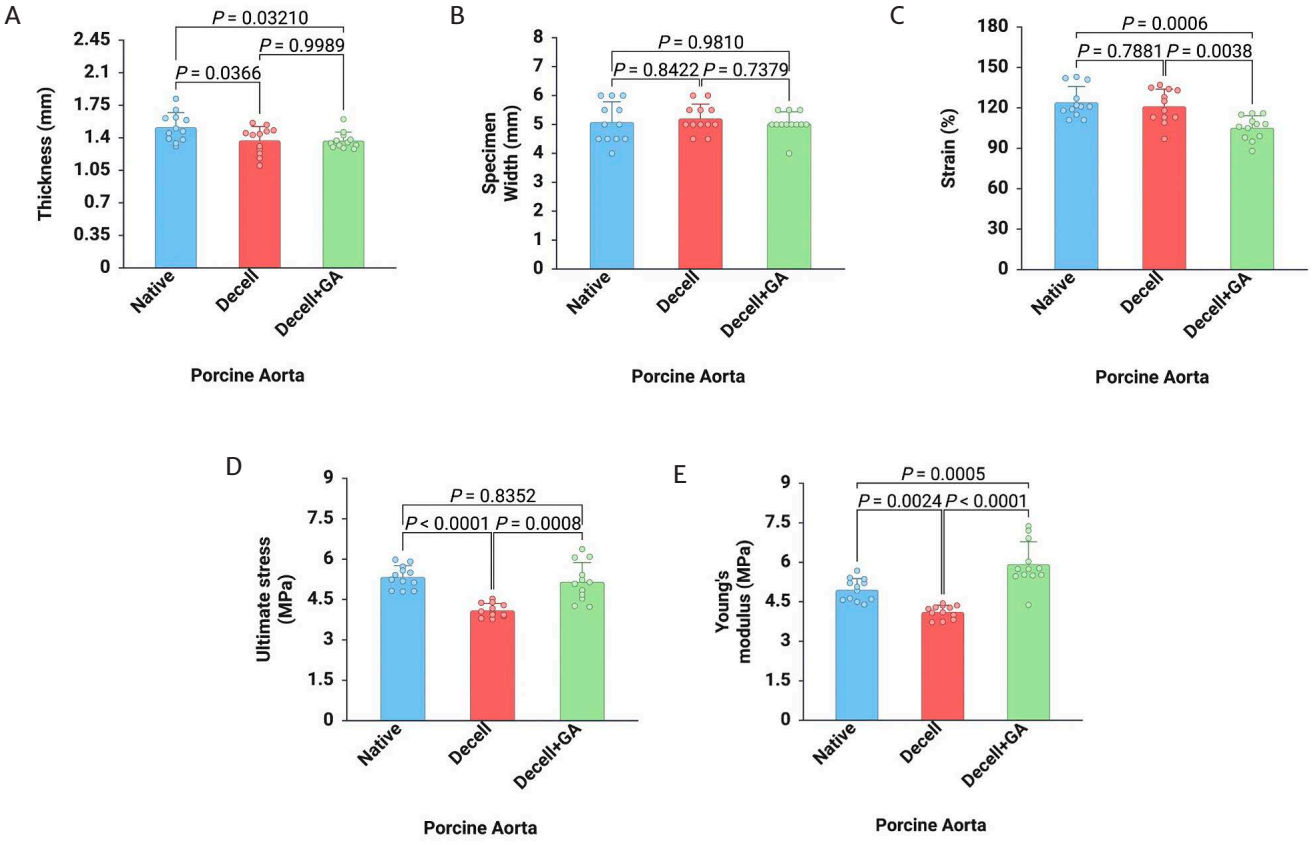

FIGURE 2. Geometric and mechanical properties of native, decellularized, and GA-crosslinked porcine aortic specimens. (**A**) Wall thickness; (**B**) width; (**C**) ultimate (failure) stress; (**D**) failure strain; (**E**) elastic modulus.

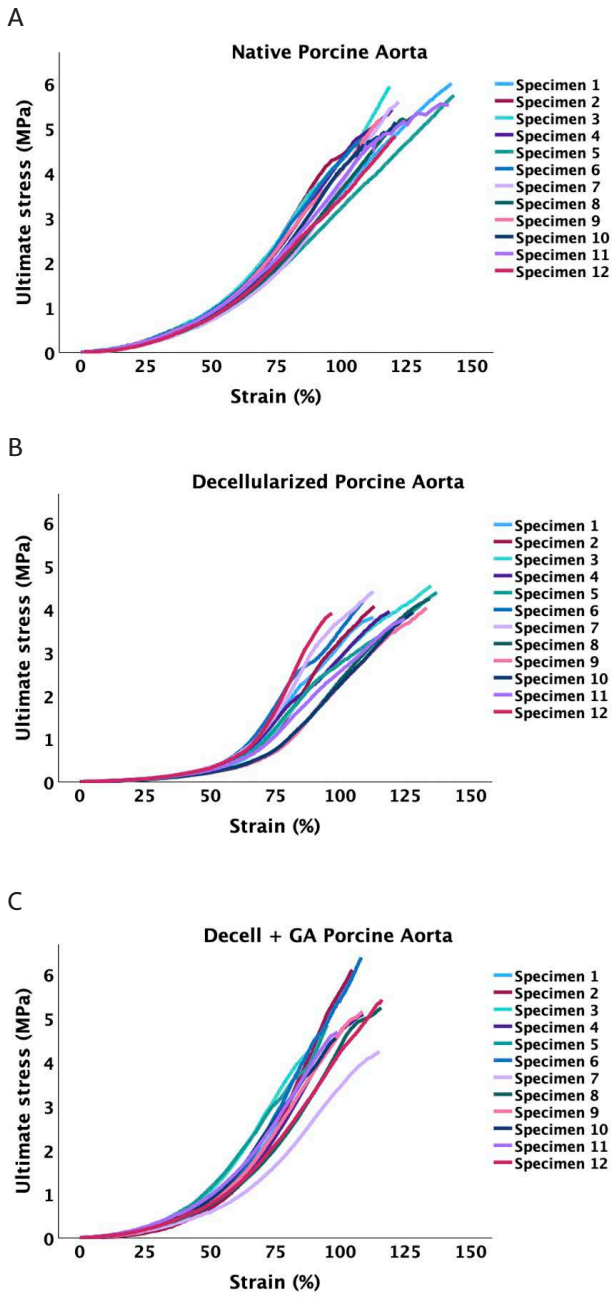

FIGURE 3. Representative uniaxial stress–strain curves for native, decellularized, and decellularized-plus-crosslinked (Decell+GA) porcine aortic specimens, illustrating the J-shaped hyperelastic response.

ing-dependent pattern. Strain at failure was preserved after decellularization ($p = 0.7881$) but fell significantly after crosslinking, relative to both native tissue ($p = 0.0006$) and the decellularized group ($p = 0.0038$) (Figure 2). Correspondingly, Young's modulus was lowest in the decellularized group, significantly below native ($p = 0.0024$), and rose markedly after crosslinking to exceed both the decellularized ($p < 0.0001$) and native ($p = 0.0005$) values (Figure 2).

The specimen-level stress–strain curves (Figure 3) were consistent with these group-level metrics. Native specimens exhibited the characteristic J-shaped response of the arterial wall, with a compliant low-strain toe region followed by progressive stiffening, reaching peak stresses at strains of 110–140% (Figure 3). Decellularized specimens retained the overall non-linear profile but displayed a delayed, more abrupt transition into the stiff collagen-dominated region and clustered at lower peak stresses (Figure 3), reflecting the reduction in ultimate strength quantified in Figure 2 and Table 1. After GA crosslinking, the curves shifted upward and to the left, with steeper terminal slopes and peak stresses returning to the native range, but failure occurring at lower strains (Figure 3), consistent with the increased modulus and reduced extensibility observed at the group level.

H&E staining confirmed effective decellularization with preservation of matrix architecture (Figure 4). The native aortic wall showed densely packed eosinophilic collagen and elastin fibers interspersed with numerous elongated basophilic nuclei aligned along the fiber axis (Figure 4). After perfusion-based decellularization, nuclei were absent throughout the wall, indicating comprehensive removal of cellular material (Figure 4). This clearance was achieved without matrix collapse: the eosinophilic fibrillar network remained intact and retained its native wavy organization, albeit with a looser, more porous architecture and enlarged interfibrillar spaces, an expected consequence of cell extraction.

DISCUSSION

This study demonstrates that a rapid perfusion-based decellularization protocol using sequential 1% Triton X-100 and 1% SDS produces structurally modified porcine aortic scaffolds whose mechanical properties are substantially restored and, in some respects, enhanced by subsequent GA crosslinking. Three findings stand out: decellularization reduced wall thickness and impaired tensile strength and stiffness; crosslinking restored ultimate stress to native levels and raised stiffness above native values; and failure strain, preserved through decellularization, was significantly reduced by crosslinking, reflecting a trade-off between structural reinforcement and extensibility. These observations are considered below against the literature on decellularized scaffolds, crosslinking strategies, and the biomechanical requirements of large-diameter grafts.

The reduction in wall thickness ($p = 0.0366$) is consistent with removal of cellular mass and disruption of extracellular-matrix microarchitecture reported after deter-

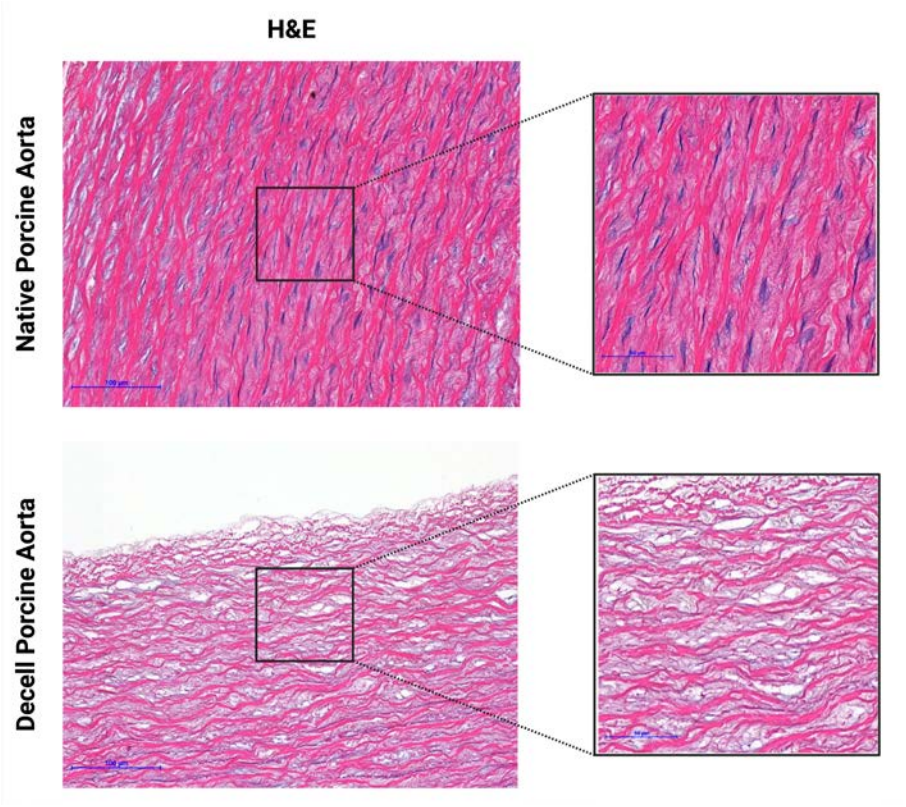

FIGURE 4. Histological confirmation of decellularization. Representative H&E-stained sections of native and decellularized porcine thoracic aorta. Boxed regions are shown at higher magnification on the right. Scale bars: 100 µm (left) and 50 µm (right).

gent processing of vascular tissue.[27-29] The accompanying falls in ultimate stress ($p < 0.0001$) and Young's modulus ($p = 0.0024$) are in keeping with disruption of collagen-fiber organization and loss of cellular load-bearing, and they mirror the extended toe region and lower peak stresses seen in the decellularized stress–strain curves. Importantly, failure strain was preserved, indicating that the scaffold retains the extensibility needed for anastomotic suturing and accommodation of pulsatile loads.

A central challenge in decellularized scaffold development is that processing conditions influence the degree of extracellular matrix disruption.[27-29] The rapid protocol used here – sequential anionic (SDS) and non-ionic (Triton X-100) detergents under perfusion – was designed to minimize processing time while achieving cell removal, reflecting the clinical priority of rapid scaffold availability in trauma. The mechanical changes observed are consistent with the known denaturing effect of SDS on collagen crosslinks and proteoglycan content; correlating these changes with specific matrix alterations will require histological and biochemical characterization of residual DNA, collagen architecture, and glycosaminoglycan content.

Crosslinking, however, significantly reduced failure strain (Figure 2D), denoting a meaningful loss of extensibility. Reduced compliance is a recognized consequence of GA fixation and has clinical relevance, given that compliance mismatch at anastomoses is a key driver of neointimal hyperplasia and mid-term failure in synthetic prostheses.[12,18] Residual cytotoxicity and a propensity for calcification are further well-documented drawbacks of GA that may impair recellularization and durability.[38,39]

More recently, our team proposed riboflavin-mediated UVA irradiation (UVA/R) as a novel, efficient, and safe crosslinking method for cardiovascular tissue.[37,40-43]

The biomechanical profile of the crosslinked porcine aortic scaffold, with ultimate stress restored to native levels and stiffness exceeding that of native tissue, suggests that the construct possesses the tensile integrity required to withstand arterial hemodynamic loading and suturing forces, addressing key biomechanical prerequisites for vascular graft function.[19] From a clinical perspective, the large caliber of the porcine aorta makes it inherently suited as a large-diameter conduit, circumventing the diameter mismatch that precludes use of the saphenous vein for aortic or iliac reconstruction.[12] Its biological composi-

tion may also confer resistance to infection in contaminated traumatic wounds, where prosthetic graft infection remains a feared complication requiring surgical explantation and carrying substantial mortality.[16,20,21] The rapid decellularization protocol used here is consistent with the operational constraints of damage-control surgery, where minimizing time to reconstruction is essential.

A key theoretical advantage over ePTFE and Dacron is the potential for host cell infiltration and progressive tissue remodeling enabled by the preserved extracellular matrix scaffold.[22-24] If recellularization and endothelialization occur in vivo, the risk of neointimal hyperplasia, the primary mechanism of synthetic graft failure, may be substantially reduced.[18]

Beyond emergency large-vessel trauma, a decellularized, crosslinked TEVG holds promise across several vascular reconstruction settings where conventional conduits fall short.[44-47] It offers a valuable alternative when no suitable autologous vein is available – whether consumed by prior bypass, of inadequate caliber, or absent – and avoids the long-term mechanical fatigue and infection susceptibility that limit synthetic grafts.[45] Such a biological, recellularization-competent conduit is equally advantageous in oncovascular surgery, where en bloc tumor resection mandates segmental venous or arterial reconstruction in patients with abdominal aortic aneurysm, often in contaminated or irradiated fields,[46,47] and in hemodialysis access reconstruction, where infection resistance and the avoidance of additional venous harvest are particularly desirable.[44] This hypothesis requires validation in long-term in vivo models, and long-term patency data will be essential before clinical translation can be considered.

A further consideration specific to xenogeneic scaffolds is residual immunogenicity, dominated by the galactose-α1,3-galactose (alpha-Gal) epitope, against which humans carry high-titer natural antibodies and which drives hyperacute rejection of unmodified porcine tissue.[48] Two aspects of the present protocol are relevant. Perfusion decellularization, and anionic detergents such as SDS in particular, substantially reduce alpha-Gal burden, yet decellularization alone does not eliminate alpha-Gal or the spectrum of non-Gal xenoantigens retained within the extracellular matrix, therefore scaffold acellularity cannot be equated with immunological acceptability.[49] GA crosslinking attenuates antigen presentation largely by masking rather than removing epitopes; residual alpha-Gal has been quantified even in clinically implanted GA-fixed bioprostheses and has been implicated in calcification and structural degeneration.[50]

LIMITATIONS

The present study has several limitations. The mechanical evaluation was limited to uniaxial tensile testing, which does not fully replicate the multiaxial stress state experienced by arterial grafts under pulsatile hemodynamic loading; suture retention strength, burst pressure, and compliance under physiological pressures were not assessed. Decellularization was not histologically or biochemically verified in the current report, and quantification of residual DNA content, collagen architecture, and glycosaminoglycan preservation will be required to confirm scaffold quality. The study was performed ex vivo, and in vivo host response, remodeling capacity, and long-term patency remain to be evaluated. The absence of standardized testing protocols for large-diameter TEVGs further complicates direct cross-study comparison and underscores the need for consensus methodology in this emerging field.

CONCLUSIONS

This preliminary study demonstrates that rapid perfusion-based decellularization of porcine aortic tissue, followed by GA crosslinking, produces large-diameter scaffolds with tensile strength restored to native levels and stiffness above native values, supporting their structural suitability as vascular conduits. These results establish a biomechanical foundation for further development of decellularized porcine aortic scaffolds as off-the-shelf large-diameter TEVGs, with future studies required to assess in vivo performance, host remodeling, long-term patency, and infection resistance in preclinical models.

CONFLICT OF INTEREST

Nothing to declare.

FUNDING

This work was supported by the George Emil Palade University of Medicine, Pharmacy, Sciences and Technology of Târgu Mureș, research grant no. 5955/1/17.06.2024.

AUTHOR CONTRIBUTIONS

B.I.L., P.A.I. and E.M.A. conceptualized the study, developed the methodology and prepared the original draft of the manuscript.. B.I.L., C.C.C., A.M., P.A.I., E.M.A. and M.A.B. conducted the investigation and performed the experimental procedures, including tissue harvesting, decellularization, crosslinking, histological processing, and

biomechanical testing. E.M.A. contributed to formal analysis and interpretation of the data. B.I.L., C.C.C. and P.B. curated the data. E.M.A., R.B., A.V.M. and E.R. reviewed and edited the manuscript. All authors contributed to visualization. R.B., A.V.M. and E.R. supervised the study, provided resources and project administration and acquired funding. All authors have read and agreed to the published version of the manuscript.

REFERENCES

1. Wahlgren CM, Aylwin C, Davenport RA, et al. Editor's Choice – European Society for Vascular Surgery (ESVS) 2025 Clinical Practice Guidelines on the Management of Vascular Trauma. Eur J Vasc Endovasc Surg. 2025;69(2):179-237. doi: 10.1016/j.ejvs.2024.12.018
2. Johannesdottir BK, Geisner T, Gubberud ET, Gudbjartsson T. Civilian vascular trauma, treatment and outcome at a level 1-trauma centre. Scand J Trauma Resusc Emerg Med. 2022;30(1):74. doi: 10.1186/s13049-022-01059-5
3. Faulconer ER, Branco BC, Loja MN, et al. Use of open and endovascular surgical techniques to manage vascular injuries in the trauma setting: A review of the American Association for the Surgery of Trauma PROspective Observational Vascular Injury Trial registry. J Trauma Acute Care Surg. 2018;84(3):411-417. doi: 10.1097/TA.0000000000001776
4. Demetriades D, Velmahos GC, Scalea TM, et al. Operative repair or endovascular stent graft in blunt traumatic thoracic aortic injuries: results of an American Association for the Surgery of Trauma Multicenter Study. J Trauma. 2008;64(3):561-570; discussion 570-571. doi: 10.1097/TA.0b013e3181641bb3
5. Richmond BK, Judhan R, Sherrill W, et al. Trends and Outcomes in the Operative Management of Traumatic Vascular Injuries: A Comparison of Open versus Endovascular Approaches. Am Surg. 2017;83(5):495-501.
6. Stonko DP, Azar FK, Betzold RD, et al. Contemporary Management and Outcomes of Injuries to the Inferior Vena Cava: A Prospective Multicenter Trial From PROspective Observational Vascular Injury Treatment. Am Surg. 2023;89(4):714-719. doi: 10.1177/00031348211038556
7. Karaolanis G, Moris D, McCoy CC, Tsilimigras DI, Georgopoulos S, Bakoyiannis C. Contemporary Strategies in the Management of Civilian Abdominal Vascular Trauma. Front Surg. 2018;5:7. doi: 10.3389/fsurg.2018.00007
8. Branco BC, Boutrous ML, DuBose JJ, et al. Outcome comparison between open and endovascular management of axillosubclavian arterial injuries. J Vasc Surg. 2016;63(3):702-709. doi: 10.1016/j.jvs.2015.08.117
9. Singh N, Quan RW. 18 - Damage Control: Considerations for Vascular Conduit in the Repair of Vascular Injury. In: Rasmussen TE, Tai NRM, eds. Rich's Vascular Trauma (Third Edition). Elsevier; 2016:206-214. doi: 10.1016/B978-1-4557-1261-8.00018-7
10. Pennel T, Zilla P. Clinical Applications and Limitations of Vascular Grafts. In: Tissue-Engineered Vascular Grafts. Springer, Cham; 2020:3-34. doi: 10.1007/978-3-030-05336-9_1
11. Pashneh-Tala S, MacNeil S, Claeyssens F. The Tissue-Engineered Vascular Graft-Past, Present, and Future. Tissue Eng Part B Rev. 2016;22(1):68-100. doi: 10.1089/ten.teb.2015.0100
12. Wilson John N, Dang C, Reddy N, Chao C, Ho KJ, Jiang B. Bioengineering Strategies for Treating Neointimal Hyperplasia in Peripheral Vasculature: Innovations and Challenges. Adv Healthc Mater. 2025;14(7):e2401056. doi: 10.1002/adhm.202401056
13. Spudil V, Hána L, Pohnán R. Peripheral vascular trauma – basic management, diagnosis and treatment. Rozhl Chir. 2023;102(8):315-320. doi: 10.33699/PIS.2023.102.8.315-320
14. Fox LCJ, Kreishman MP. High-Energy Trauma and Damage Control in the Lower Limb. Semin Plast Surg. 2010;24(1):5-10. doi: 10.1055/s-0030-1253241
15. Keck KJ, Adams TJ, Day KM. Radial Recurrent Artery: Autologous Patch Graft for Acute Brachial Artery Laceration. Cureus. 12(9):e10682. doi: 10.7759/cureus.10682
16. Chakfé N, Diener H, Lejay A, et al. Editor's Choice – European Society for Vascular Surgery (ESVS) 2020 Clinical Practice Guidelines on the Management of Vascular Graft and Endograft Infections. Eur J Vasc Endovasc Surg. 2020;59(3):339-384. doi: 10.1016/j.ejvs.2019.10.016
17. Szafron JM, Heng EE, Boyd J, Humphrey JD, Marsden AL. Hemodynamics and Wall Mechanics of Vascular Graft Failure. Arteriosclerosis, Thrombosis, and Vascular Biology. 2024;44(5):1065-1085. doi: 10.1161/ATVBAHA.123.318239
18. Zain MA, Jamil RT, Siddiqui WJ. Neointimal Hyperplasia. In: StatPearls. StatPearls Publishing; 2023. Accessed January 29, 2026. Available from http://www.ncbi.nlm.nih.gov/books/NBK499893/
19. Jarad NA, Chami A, Weitz JI, Didar TF. Advancements in surface modification strategies of vascular grafts to improve biocompatibility and tissue integration. Explor BioMat-X. 2024;1(5):241-265. doi: 10.37349/ebmx.2024.00018
20. He E, Serpelloni S, Alvear P, Rahimi M, Taraballi F. Vascular Graft Infections: An Overview of Novel Treatments Using Nanoparticles and Nanofibers. Fibers. 2022;10(2):12. doi: 10.3390/fib10020012
21. Kirkton RD, Prichard HL, Santiago-Maysonet M, Niklason LE, Lawson JH, Dahl SLM. Susceptibility of ePTFE vascular grafts and bioengineered human acellular vessels to infection. J Surg Res. 2018;221:143-151. doi: 10.1016/j.jss.2017.08.035
22. Lopera Higuita M, Griffiths LG. Small Diameter Xenogeneic Extracellular Matrix Scaffolds for Vascular Applications. Tissue Engineering Part B: Reviews. 2020;26(1):26-45. doi: 10.1089/ten.teb.2019.0229
23. Massaro MS, Kochová P, Pálek R, et al. Decellularization of Porcine Carotid Arteries: From the Vessel to the High-Quality Scaffold in Five Hours. Front Bioeng Biotechnol. 2022;10. doi: 10.3389/fbioe.2022.833244
24. Leal BBJ, Wakabayashi N, Oyama K, Kamiya H, Braghirolli DI, Pranke P. Vascular Tissue Engineering: Polymers and Methodologies for Small Caliber Vascular Grafts. Front Cardiovasc Med. 2021;7. doi: 10.3389/fcvm.2020.592361
25. Ding H, Hou X, Gao Z, Guo Y, Liao B, Wan J. Challenges and Strategies for Endothelializing Decellularized Small-Diameter Tissue-Engineered Vessel Grafts. Advanced Healthcare Materials. 2024;13(16):2304432. doi: 10.1002/adhm.202304432
26. Lang Z, Chen T, Zhu S, et al. Construction of vascular grafts based on tissue-engineered scaffolds. Mater Today Bio. 2024;29:101336. doi: 10.1016/j.mtbio.2024.101336
27. Aldridge A, Desai A, Owston H, et al. Development and characterisation of a large diameter decellularised vascular

allograft. Cell Tissue Bank. 2018;19(3):287-300. doi: 10.1007/s10561-017-9673-y
28. Giovanniello F, Asgari M, Breslavsky ID, et al. Development and mechanical characterization of decellularized scaffolds for an active aortic graft. Acta Biomater. 2023;160:59-72. doi: 10.1016/j.actbio.2023.02.013
29. Wu P, Nakamura N, Kimura T, et al. Decellularized porcine aortic intima-media as a potential cardiovascular biomaterial. Interact Cardiovasc Thorac Surg. 2015;21(2):189-194. doi: 10.1093/icvts/ivv113
30. Mallis P, Kostakis A, Stavropoulos-Giokas C, Michalopoulos E. Future Perspectives in Small-Diameter Vascular Graft Engineering. Bioengineering. 2020;7(4):160. doi: 10.3390/bioengineering7040160
31. Wang X, Chan V, Corridon PR. Decellularized blood vessel development: Current state-of-the-art and future directions. Front Bioeng Biotechnol. 2022;10. doi: 10.3389/fbioe.2022.951644
32. Arbănaşi EMM, Chirilă TVV. Preservation of human vascular tissue and the relevance of temperature: a narrative review. Front Bioeng Biotechnol. 2026;13. doi: 10.3389/fbioe.2025.1631214
33. Ion AP, Asztalos A, Ciucanu CC, et al. Superior Measurement Accuracy of Digital Thickness Gauge Versus Digital Vernier Caliper in Determining Venous Tissue Thickness. Cureus. 2024;16(9):e68442. doi: 10.7759/cureus.68442
34. Ciucanu CC, Russu E, Mureşan A, et al. Analysis of digital vernier caliper versus digital thickness gauge consistency and user experience in measuring arterial wall thickness: implications for biomechanical assessment. Front Bioeng Biotechnol. 2026;14. doi: 10.3389/fbioe.2026.1791599
35. Ion AP, Asztalos A, Ciucanu CC, et al. Optimizing Arterial Tissue Thickness Measurement Protocols: Digital Vernier Caliper Versus Digital Thickness Gauge. Methods and Protocols. 2024;7(6):90. doi: 10.3390/mps7060090
36. Trâmbițaș C, Cordoș BA, Dorobanțu DC, et al. Application of Adipose Stem Cells in 3D Nerve Guidance Conduit Prevents Muscle Atrophy and Improves Distal Muscle Compliance in a Peripheral Nerve Regeneration Model. Bioengineering. 2024;11(2):184. doi: 10.3390/bioengineering11020184
37. Arbănaşi EM, Russu E, Arbănaşi EM, et al. Effect of Ultraviolet Radiation on the Enzymolytic and Biomechanical Profiles of Abdominal Aortic Adventitia Tissue. Journal of Clinical Medicine. 2024;13(2):633. doi: 10.3390/jcm13020633
38. Qiao S, Peijie T, Nan J. Crosslinking strategies of decellularized extracellular matrix in tissue regeneration. Journal of Biomedical Materials Research Part A. 2024;112(5):640-671. doi: 10.1002/jbm.a.37650
39. Human P, Ofoegbu C, Ilsley H, et al. Decellularization and engineered crosslinking: a promising dual approach towards bioprosthetic heart valve longevity. Eur J Cardiothorac Surg. 2020;58(6):1192-1200. doi: 10.1093/ejcts/ezaa257
40. Russu E, Arbanasi EM, Chirila TV, Muresan AV. Therapeutic strategies based on non-ionizing radiation to prevent venous neointimal hyperplasia: the relevance for stenosed arteriovenous fistula, and the role of vascular compliance. Front Cardiovasc Med. 2024;11. doi: 10.3389/fcvm.2024.1356671
41. Chirila TV, Suzuki S. Ultraviolet-induced mechanical augmentation of the degraded porcine aortic adventitia: Its significance for preventing aneurysmal rupture. Global Translational Medicine. 2023;2(2):0897. doi: 10.36922/gtm.0897
42. Chirila TV, Suzuki S. Effects of Ultraviolet-A Radiation on Enzymatically Degraded Tunica Adventitia of the Porcine Abdominal Aorta. Biomedical Materials & Devices. 2023;1(2):1000-1008. doi: 10.1007/s44174-023-00080-1
43. Chirila TV, Suzuki S. Photocrosslinking of Adventitial Collagen in the Porcine Abdominal Aorta: A Preliminary Approach to a Strategy for Prevention of Aneurysmal Rupture. Designs. 2022;6(1):5. doi: 10.3390/designs6010005
44. Ujlaki-Nagi AA, Szanto LA, Florea E, et al. Reconstruction of a Thrombosed Aneurysmal Radio-Cephalic Arteriovenous Fistula with a Tubular Bovine Pericardial Conduit. Kidney and Dialysis. 2025;5(3):46. doi: 10.3390/kidneydial5030046
45. Arbănaşi EM, Trâmbițaș C, Ciucanu CC, et al. Giant Pseudoaneurysm as an Uncommon Late Complication Following a Fourteen-Year Femoropopliteal Bypass in a Visually Impaired Patient. Diagnostics. 2026;16(5):686. doi: 10.3390/diagnostics16050686
46. Buzgău P, Arbănași EM, Ciucanu CC, et al. Management of Great Saphenous Vein and Inferior Vena Cava Leiomyosarcomas: Two Surgical Case Reports and Literature Review. Journal of Clinical Medicine. 2026;15(4):1636. doi: 10.3390/jcm15041636
47. Russu E, Buzgău P, Ciucanu CC, et al. Preoperative nutritional status and its association with adverse events following open abdominal aortic aneurysm repair. Front Nutr. 2026;13. doi: 10.3389/fnut.2026.1776781
48. Galili U. The alpha-gal epitope and the anti-Gal antibody in xenotransplantation and in cancer immunotherapy. Immunol Cell Biol. 2005;83(6):674-686. doi: 10.1111/j.1440-1711.2005.01366.x
49. Wong ML, Griffiths LG. Immunogenicity in xenogeneic scaffold generation: antigen removal vs. decellularization. Acta Biomater. 2014;10(5):1806-1816. doi: 10.1016/j.actbio.2014.01.028
50. Naso F, Gandaglia A, Bottio T, et al. First quantification of alpha-Gal epitope in current glutaraldehyde-fixed heart valve bioprostheses. Xenotransplantation. 2013;20(4):252-261. doi: 10.1111/xen.12044